Science Translational Medicine
AAAS

stm.sciencemag.org/cgi/content/full/13/585/eaba2927/DC1

Supplementary Materials for

Citrullinated vimentin mediates development and progression of lung fibrosis

Fu Jun Li, Ranu Surolia, Huashi Li, Zheng Wang, Gang Liu, Tejaswini Kulkarni, Adriana V. F. Massicano, James A. Mobley, Santanu Mondal, Joao A. de Andrade, Scott A. Coonrod, Paul R. Thompson, Keith Wille, Suzanne E. Lapi, Mohammad Athar, Victor J. Thannickal, A. Brent Carter, Veena B. Antony*

*Corresponding author. Email: vantony@uab.edu

Published 17 March 2021, *Sci. Transl. Med.* **13**, eaba2927 (2021)
DOI: 10.1126/scitranslmed.aba2927

The PDF file includes:

Supplementary Material

Materials and Methods

TEM

To demonstrate the existence of CB in subjects from IPF or Cd/CB-treated mice, macrophages in BALF were fixed in 2.5% paraformaldehyde and 2.5% glutaraldehyde. The sections (70-80 nm) were stained with the uranyl acetate and lead citrate and imaged using a Tecnai Twin 120kv TEM (FEI) as performed described (*46*). For quantification, twenty five macrophages in each subject were counted and the percentage of CB-containing macrophages was quantified.

Vim and Cit-Vim purification

For purification of native Vim and Cit-Vim, human lung macrophages were treated with $CdCl_2$ (1.8 μg/ml) plus CB (10 μg/ml) for 48 hours. Culture supernatants were concentrated by ultrafiltration using an Amicon Ultra-15 10K centrifugal filter (Merck Millipore) and incubated with 2 μg/ml of anti-Vim antibody (Santa Cruz) or anti-Cit-Vim antibody (Cayman, clone 12G11) overnight at 4˚C. Antibody complexes were immunoprecipitated on protein A/G agarose (Santa Cruz), washed, eluted, and resolved by SDS-polyacrylamide gel electrophoresis. BCA protein assay kit (ThermoFisher) was used to determine the protein concentration. Endotoxin was evaluated using a Limulus Amebocyte Lysate test kit (Lonza) according to the manufactures' instructions.

Cit-Vim measurements by ELISA

To determine soluble Cit-Vim in lung tissue, plasma from subjects from IPF and in BALF, plasma from Cd/CB-treated mice, we developed a specific ELISA. Briefly, the EIA/RIA 96

well half-area high binding plates (Corning Costar) were coated with anti-Cit-Vim antibody (Cayman, 2.5 μg/ml) at 4°C overnight in PBS. The wells were incubated with blocking solution (1% BSA in PBS) for 2 hours at 37°C. After five washes with PBS containing 0.05% tween 20 (PBS-T), fifty microliters of diluted samples were then added and incubated for 2 hours at 37°C. After five time washes with PBS-T, the plates were incubated 1 hour at 37°C with HRP-labeled anti-Cit-Vim antibody generated using a peroxidase kit (Abcam). Fifty microliters of TMB substrate (BioLegend) A/B mixture was added and incubated for 15 min at 37°C to develop the reaction. The TMB reaction was terminated by adding fifty microliters of H_2SO_4 (1M) and O.D value at 450 nm (minus 570 nm for correction) was read using a microplate reader. The standard curve was generated by serial dilution of the purified Cit-Vim.

Immunoblot analysis

Whole cell lysates, nuclear fractionations (obtained using the NE-PER nuclear and cytoplasmic extraction kit, Pierce Biotechnology) and concentrated supernatants harvested from macrophages or fibroblasts were processed for immunoblotting according to standard procedures using the following inhibitors or primary antibodies: Calcium inhibitor CsA (Cayman Chemical); PAD2 inhibitor AFM-30a (a gift from PR. Thompson); anti-Vim, anti-collagen 1, and anti-α-SMA antibody (Santa Cruz); anti-Cit-Vim antibody (Cayman, clone 12G11); anti-metallothionein antibody (Thermo Fisher); Akt inhibitor LY294002, NF-κB inhibitor PDTC, anti-β-actin, and anti-GAPDH antibody (Sigma-Aldrich); anti-phospho-Akt1 (Ser473), anti-Akt1, anti-IκB-β, anti-phospho-IκB-β (Thr19/Ser23), and anti-p65 antibody (Cell Signaling Technology); anti-PAD4 and anti-TLR4 antibody (Abcam); anti-PAD2 antibody (Lifespan Biosciences); anti-Lamin A/C and anti-Tubulin-α antibody (BioLegend). Briefly, after electrophoresis on 4-12% gels (Bio-Rad), proteins were transferred to a PVDF

membrane (Millipore). Membranes were blocked, incubated with primary antibodies as shown above and exposed to HRP-conjugated anti-rabbit or anti-mouse antibody (Sigma-Aldrich). Images were developed and band intensities were quantitated using a Bio-Rad system.

IP-MS analysis of peptides

Cit-Vim peptides were identified and characterized by using nanoLC-ESL-MS/MS at the Mass Spectrometry/Proteomics Shared Facility in UAB as described before (*59*). Briefly, lung macrophages isolated from subjects with IPF were treated with $CdCl_2$ (1.8 μg/ml) plus CB (10 μg/ ml) and supernatants were concentrated and immunoprecipitated with anti-Vim or Cit-Vim antibodies (2 μg/ml). After immunoprecipitation with anti-Vim (Santa Cruz) or anti-Cit-Vim antibodies (Cayman, clone 12G11), the enriched elution fraction on agarose beads was eluted in 1 × LDS sample buffer at 96˚C for 10 min, denatured at 70˚C for 10 min and loaded onto a 10% Bis-tris gel. Colloidal Coomasssie was stained and the molecular weight area of interest (~54 KDa) was excised and digested with trypsin overnight. Peptide digests were injected onto an Infinity nHPLC stack (Agilent Technologies). The identified proteins were generated by using SEQUEST (Thermo Fisher) and filtered with Scaffold software (Protein Sciences).

Transwell invasion assay

Transwell chambers were used to evaluate the invasive ability of human fibroblasts. Cells (5×10^5) were seeded into the upper chamber containing 100 μl serum-free DMEM medium in the presence or absence of Vim or Cit-Vim (2.0 μg/ml), and 1 ml 10% FBS medium was added to the lower chamber. After 48 hours, the migrated cells were fixed with methanol and

stained with crystal violet (0.5%). The optical density values at 570 nm were measured as described before (*39*).

Quantitative real-time PCR (RT-PCR)

Total RNA was isolated from lung macrophages or fibroblasts using RNAqueous RNA isolation kit (Ambion) and reverse-transcribed into cDNA using iScript Reverse Transcription SuperMix for RT-qPCR according to the manufacturer's instructions (Bio-Rad). RT-PCR reactions were performed as described previously (*34*) using an SYBR Green PCR Master Mix (Applied Biosystems). Gene specific primer pairs were used: human MT-1E, 5'-GCT TGT TCG TCT CAC TGG TG-3' and 5'-CAG GTT GTG CAG GTT GTT CTA-3'; human MT-2A, 5'-CCG ACT CTA GCC GCC TCT T-3' and 5'-GTG GAA GTC GCG TTC TTT ACA-3'; human Col1a1, 5'-ACG AAG ACA TCC CAC CAA TCA CCT-3' and 5'-AGA TCA CGT CAT CGC ACA ACA CCT-3'; human Col3a1, 5'-ACA GCC TCC AAC TGC TCC TA-3' and 5'-GTC ACC ATT TCT CCC AGG AA-3'; and human β-actin, 5'-TGC TAT CCA GGC TGT GCT AT-3' and 5'-AGT CCA TCA CGA TGC CAG T-3'. Data were normalized to β-actin and calculated using the cycle threshold method.

Measurements of respiratory mechanics

To perform respiratory mechanics analysis, *PAD2*$^{-/-}$ and WT mice were anesthetized using xylazine (5 mg/kg) and ketamine (130 mg/kg) 14 days after Sal or $CdCl_2$ (0.16 mg/kg) plus CB (5.0 mg/kg) administration. After performing a tracheotomy and cannulating the trachea, mice were connected to a computer-controlled mechanical ventilator (FlexiVent, SCIREO, Montreal, Canada) via the Y-tubing supported by FlexiWare 8 software and mechanically ventilated at 150 breaths/min, tidal volume of 10 ml/kg, and a positive end-expiratory pressure of 3 cmH_2O. ECG was recorded permanently to monitor the heart rate. Mice were

paralyzed with 1.0 mg/kg of pancuronium bromide (Hospira) and then challenged with increasing concentrations of methacholine aerosol (0, 5, 10, 20, 40 mg/ml). Deep inflation perturbation (27 cmH_2O) was performed to verify the cannula insertion and attachment and PVs-P (27 cmH_2O) protocol was applied to confirm the absence of spontaneous inspiratory efforts. The scripts used in the current study included SnapShot-150 (10 ml/kg), Quick Prime-3 (3 ml/kg), Mouse Mechanics Scan and Mouse inhaled Dose Response. Parameters including Static compliance (Cst), compliance independent of weight (K) and inspiratory capacity (A) were evaluated using the PV-Loop Salazar Knowles equation. Airway resistance (Rrs) was determined using the single-compartment model. Central airway resistance (Rn), tissue resistance (G) and tissue stiffness (H) were measured by applying the constant-phase model.

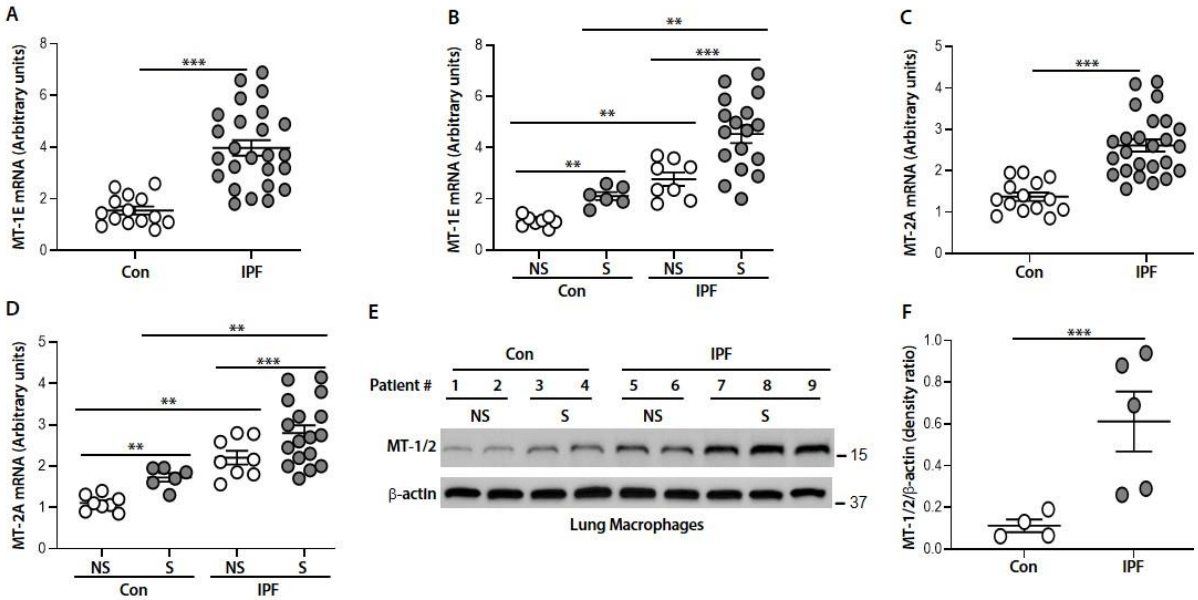

Fig. S1. MT-1/2 mRNA and protein expression is higher in subjects with IPF, especially smokers. mRNA expression in lung macrophages from control (n=14, including 8 never-smoker and 6 smoker) and IPF (n=25, including 8 never-smoker and 17 smoker) for (**A, B**) MT-1E and (**C, D**) MT-2A. (**E**) Immunoblot analysis of MT-1/2 in lung macrophage from control never-smoker (n=2), control smoker (n=2), IPF never-smoker (n=2) and IPF smoker (n=3). (**F**) Quantification of MT-1/2 from (**E**). Each dot represents an individual subject. ** $P < 0.01$; *** $P < 0.001$ using two-tailed *t* test for (**A**), (**C**) and (**F**) and one-way ANOVA followed by Tukey's post-hoc analysis for (**B**) and (**D**).

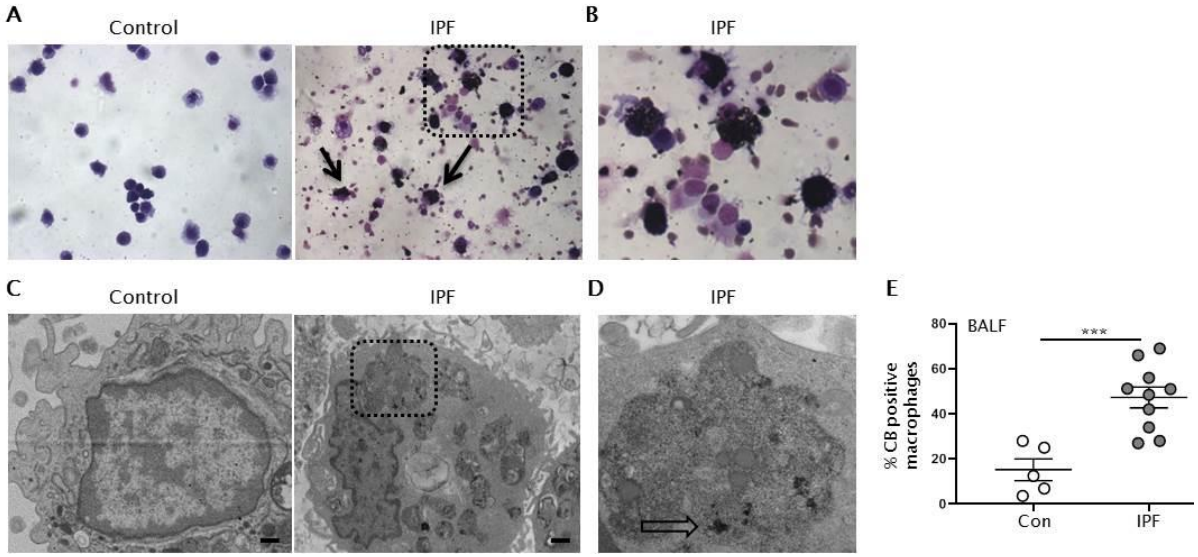

Fig. S2. CB deposits are found in macrophages from subjects with IPF. (**A**) HEMA 3 stained BALF cells and (**B**) higher magnification of inset from (**A**). Arrows indicate the stained macrophages. (**C**) Deposition of CB particles in lung macrophages as detected by TEM and (**D**) higher magnification of inset from (**C**). Open arrow indicates the particles. Scale bars, 500 nM. (**E**) Quantification of CB positive macrophages from BALF as detected by TEM. Twenty five macrophages for each subjects were counted for quantification. Data

shown are representative of experiments from control (n=5) and subjects with IPF (n=10). *** $P < 0.001$ using two-tailed *t* test.

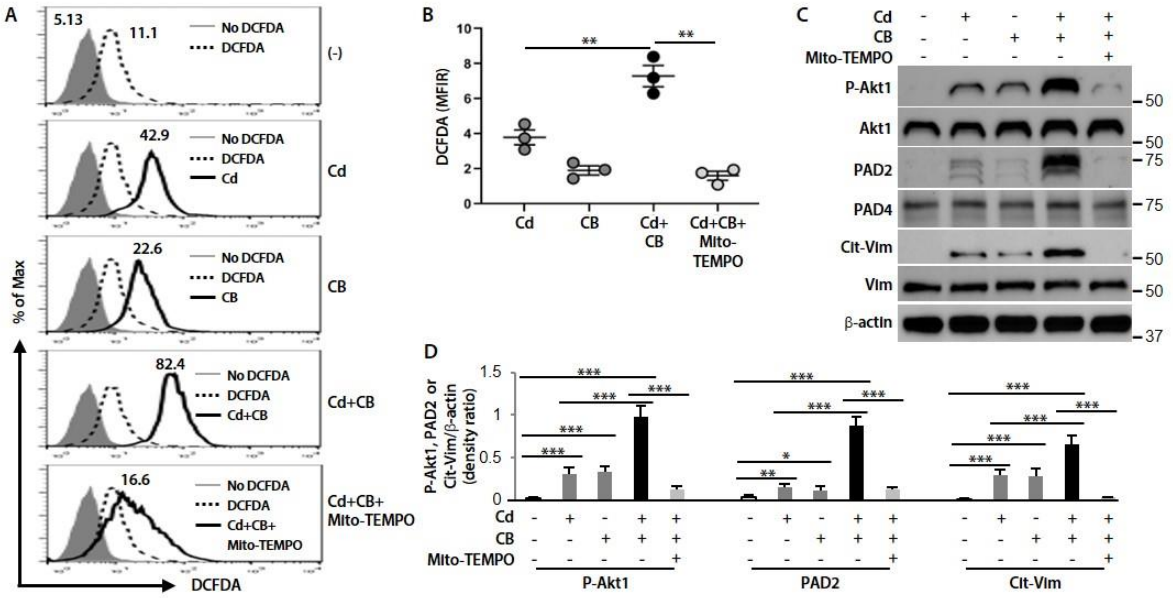

Fig. S3. Cd/CB-induced Akt1, PAD2 activation, and Vim citrullination are dependent on oxidative states. Primary human lung macrophages isolated from subjects with IPF were labeled with 20 μM DCFDA for 30 minutes and cultured for an additional 2 hours with $CdCl_2$ (1.8 μg/ml) and/or CB (10 μg/ml) in the presence or absence of Mito-TEMPO (10 μM). (**A**) Representative histograms on flow cytometry with the mean fluorescence intensity (MFI) for each condition. Data shown are representative of three experiments. (**B**) Quantification of DCFDA expression using the MFI ratio (MFIR) calculated by dividing the MFI of Cd, CB, Cd+CB or Cd+CB+Mito-TEMPO (solid line) by the MFI of DCFDA (dashed line), respectively. (**C**) Immunoblot analysis in human lung macrophages treated with $CdCl_2$ and/or CB for 2 hours in the presence or absence of Mito-TEMPO. (**D**) Quantification of P-Akt1, PAD2 and Cit-Vim from (**C**) (n=3). * $P < 0.05$; ** $P < 0.01$; *** $P < 0.001$ using one-way ANOVA followed by Tukey's post-hoc analysis.

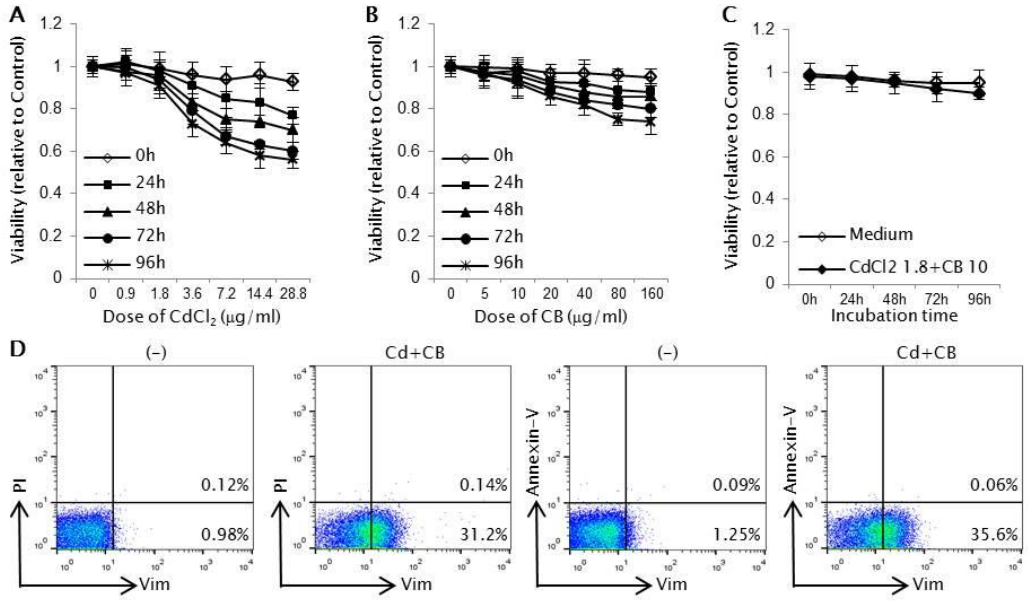

Fig. S4. Cells that express Vim on their surface are not apoptotic. Primary human lung macrophages isolated from subjects with IPF were cultured with (**A**) $CdCl_2$ (0.9 to 28.8 μg/ml) (**B**) CB (5 to 160 μg/ml), or (**C**) $CdCl_2$ (1.8 μg/ml) plus CB (10 μg/ml). Cell viability relative to control was shown and evaluated by using MTT (Sigma-Aldrich) assay (*7*). MTT (5 mg/ml) was added for additional 4 hours prior to addition of DMSO. Values shown as mean ± S.E.M. (**D**) Representative histograms on flow cytometry performed on primary human lung macrophages that were cultured in the presence or absence of $CdCl_2$ (1.8 μg/ml) plus CB (10 μg/ml) for 48 hours. Cells were then stained with PI, anti-Annexin V-FITC and Vim-PE. Flow cytometry dot plots for the simultaneous binding of Vim and PI or Annexin V uptake were shown. Data shown are representative of three independent experiments.

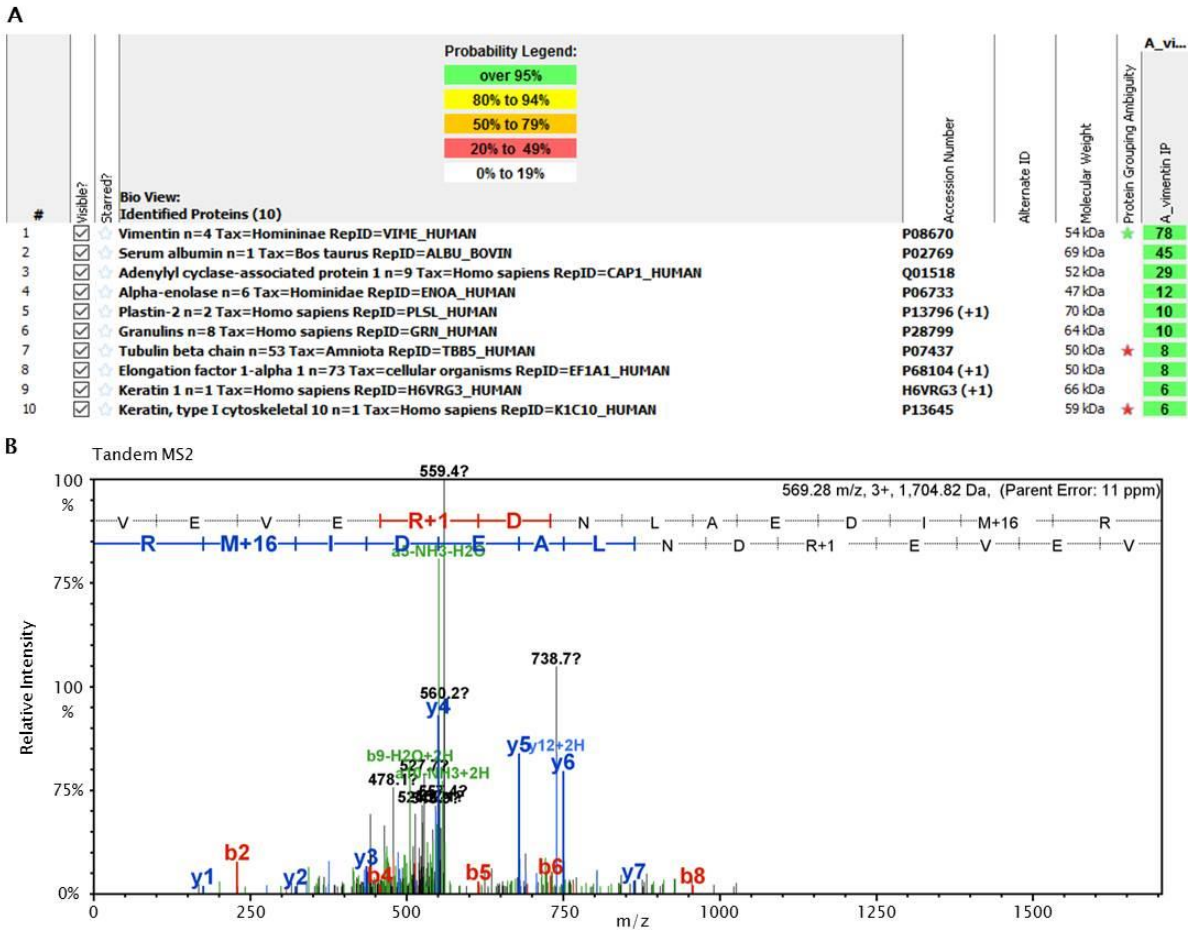

Fig. S5. Proteins are identified and tandem MS2 spectrum is characterized by IP-MS. The concentrated supernatants of lung macrophages isolated from subjects with IPF were immunoprecipitated with anti-Vim or Cit-Vim antibodies and IP samples on agarose beads were loaded onto a 10% Bis-tris gel after denaturation. The interested molecular weight areas were excised and digested with trypsin overnight prior to MS analysis for the citrullinated cites. (**A**) List of proteins identified with filters, ≥ 99% protein probability, ≥ 5 peptides, and ≥ 95% peptide probability. This table demonstrates as a proof of principal, the relative quantitative values (i.e. total spectrum counts shown in green) measured using MS for each identified protein that was identified in the IP pull-down. (**B**) The resulting tandem MS2 spectrum for the tryptic peptide.

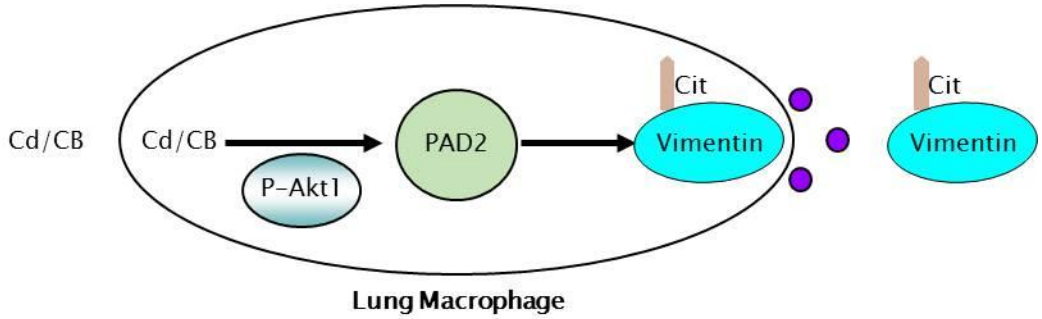

Fig. S6. Schematic diagram of the Cit-Vim secretion pathway.

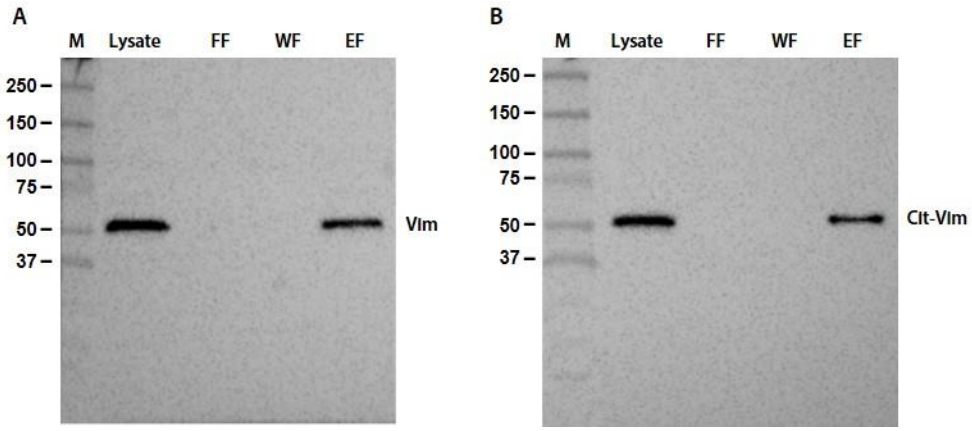

Fig. S7. Both Vim and Cit-Vim are purified and enriched from cell culture supernatants. Primary human lung macrophages were cultured with $CdCl_2$ (1.8 μg/ml) plus CB (10 μg/ml) and recovered for 48 hours and supernatants were concentrated, immunoprecipitated with (**A**) anti-Vim or (**B**) Cit-Vim antibodies (Cayman, clone 12G11), followed by enrichment procedures using protein A/G plus-agarose beads as described previously (*36*). Equal aliquots of 30 μg protein per lane were added and analyzed by western blotting using indicated antibodies. The non-enriched total cell lysate was used as a control. FF = flow-through fraction, WF = wash fraction and EF = elution fraction.

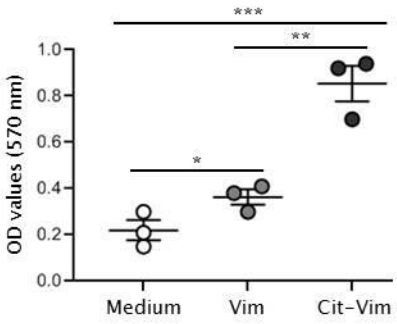

Fig. S8. Cit-Vim exposure induces more invasive subtypes of fibroblasts. Primary human lung fibroblasts (5×10^5) isolated from normal subjects were incubated for 48 hours in the presence of Vim or Cit-Vim (2 μg/ml) and the invasive ability of fibroblasts were evaluated using the transwell assay. Data shown are representative of three independent experiments from three individual subjects * $P < 0.05$; ** $P < 0.01$; *** $P < 0.001$ using one-way ANOVA followed by Tukey's post-hoc analysis.

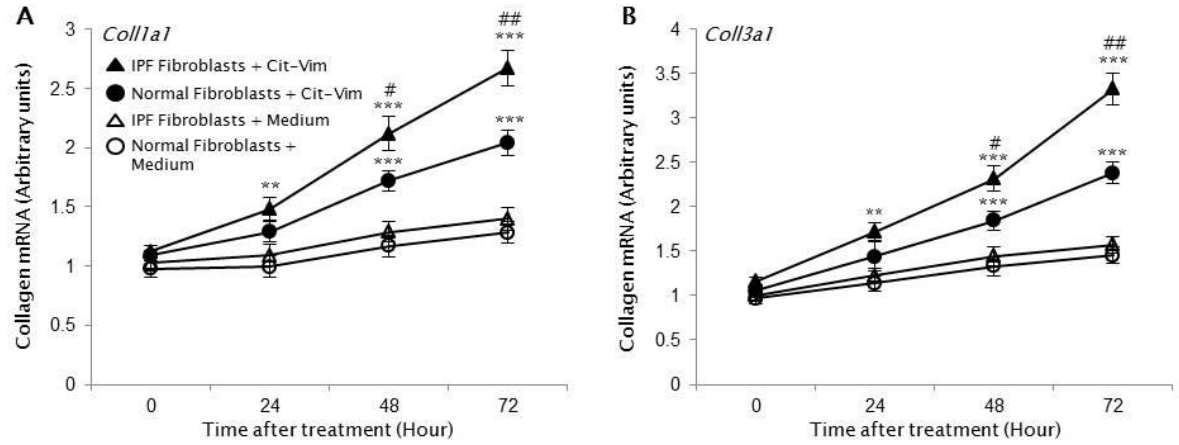

Fig. S9. Cit-Vim exposure enhances the expression of collagen in fibroblasts isolated from normal subjects and subjects with IPF. Primary human lung fibroblasts (5×10^5/ml) isolated from normal or subjects with IPF were incubated with or without Cit-Vim (2 μg/ml). (**A**) *Col1α1* and (**B**) *Col3α1* mRNA expression in fibroblasts stimulated with Cit-Vim at different time points. Data shown represent the mean values of three independent experiments from three individual subjects. ** $P < 0.01$; *** $P < 0.001$ vs 0 hour and $^{\#}P < 0.05$; $^{\#\#}P <$

0.01 vs normal fibroblasts + Cit-Vim at 48 or 72 hour using one-way ANOVA followed by Tukey's post-hoc analysis.

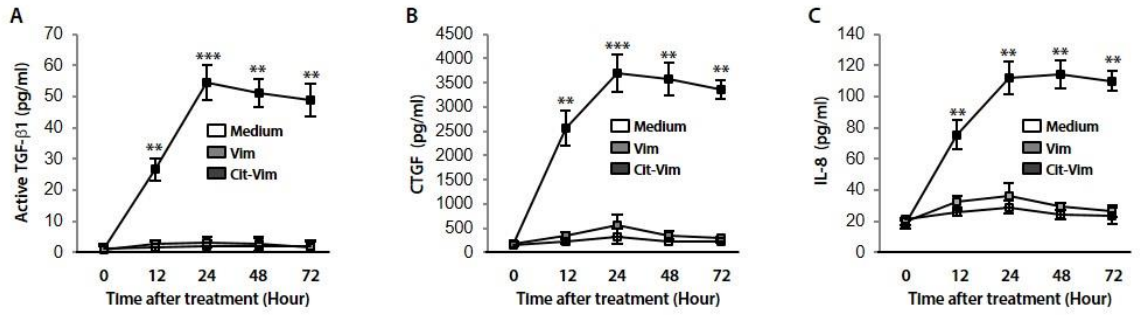

Fig. S10. Cit-Vim, but not Vim, induces CTGF, IL-8, and active TGF-β1 production. Primary human lung fibroblasts (5×10^5/ml) isolated from normal subjects were treated with Vim or Cit-Vim (2 μg/ml) for different time points. The concentrations of (**A**) active TGF-β1, (**B**) CTGF and (**C**) IL-8 in the supernatants were measured by ELISA. ** $P < 0.01$; *** $P < 0.001$ vs 0 hour using one-way ANOVA followed by Tukey's post-hoc analysis.

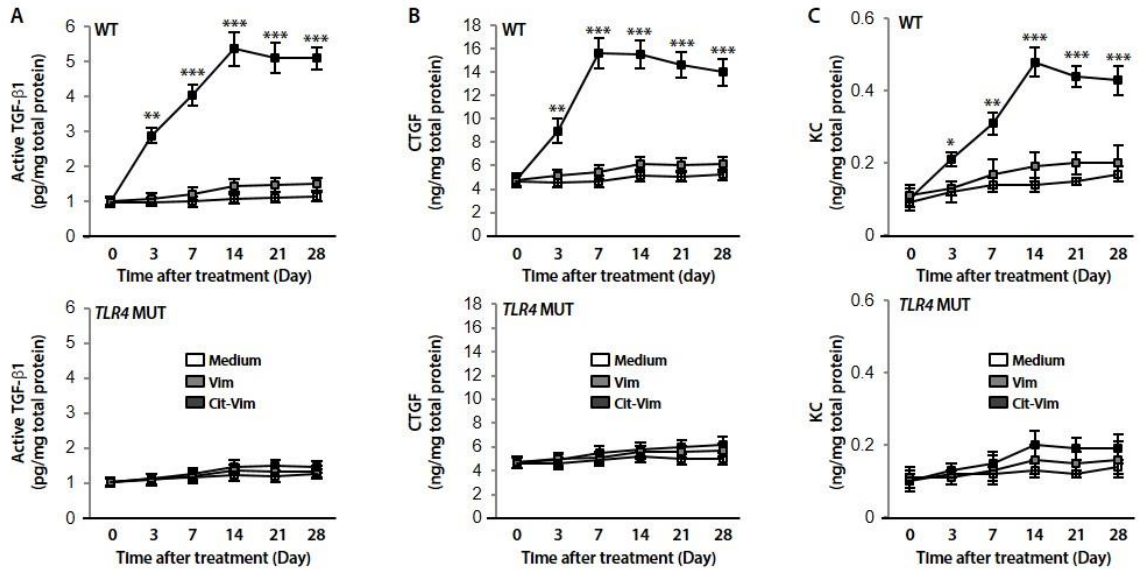

Fig. S11. Cit-Vim, but not Vim, can effectively induce cytokine/chemokine production only in TLR4 WT mice. TLR4 WT or *TLR4* MUT mice (n=5 per group) were treated intratracheally with Vim or Cit-Vim (2 mg/kg) for different time points. Each dot represents an individual mouse. The concentrations of (**A**) active TGF-β1, (**B**) CTGF and (**C**) KC in lung tissue suspensions were measured by ELISA. * $P < 0.05$; ** $P < 0.01$; *** $P < 0.001$ vs 0 day using one-way ANOVA followed by Tukey's post-hoc analysis.

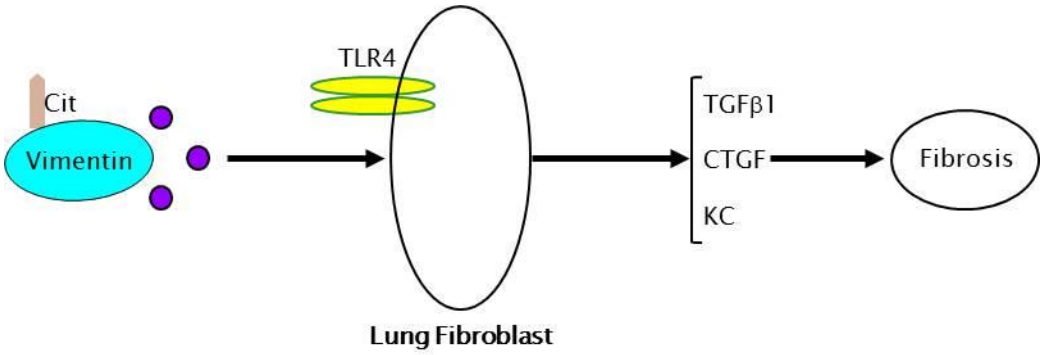

Fig. S12. Schematic diagram of the Cit-Vim–induced fibrosis pathway.

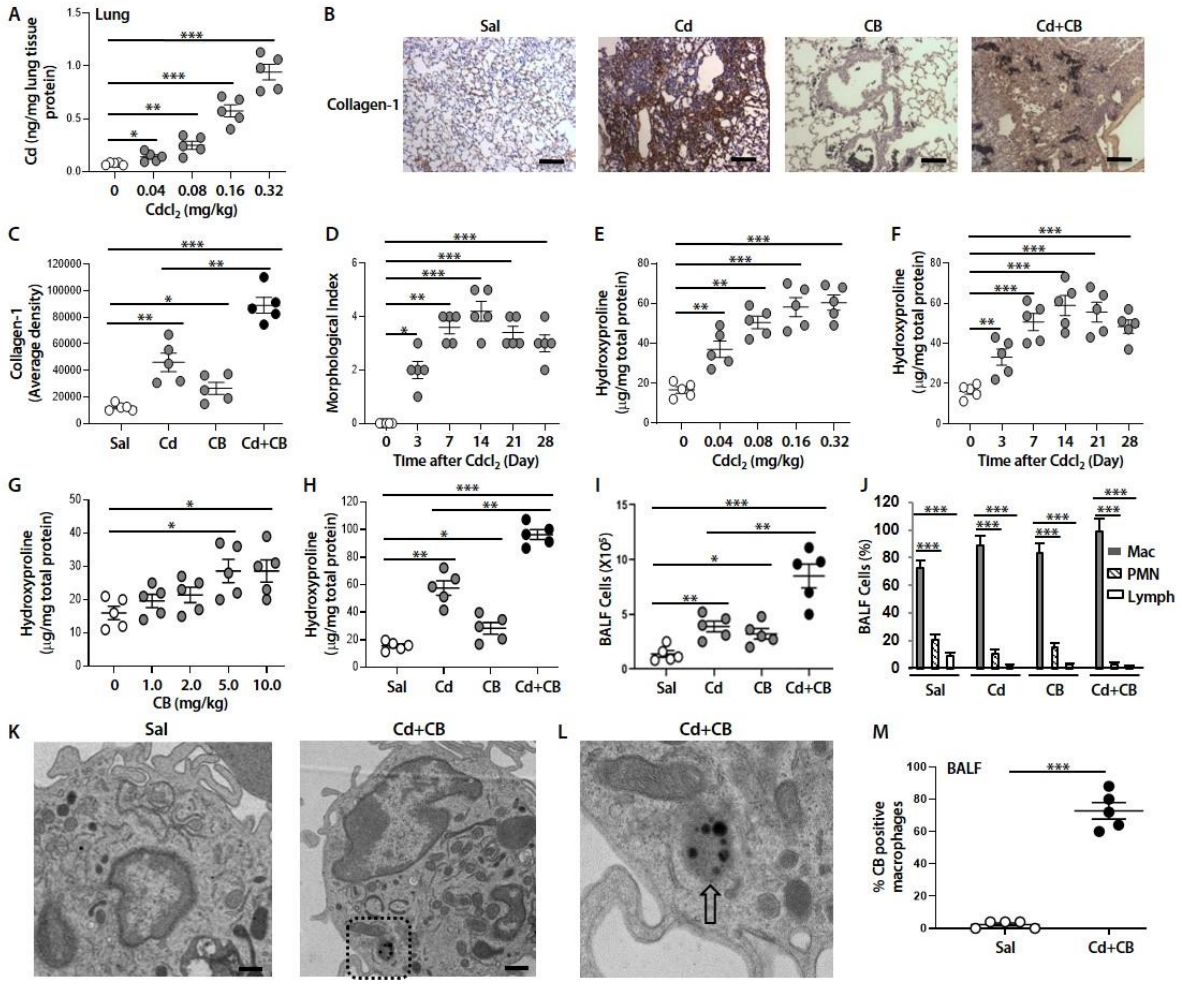

Fig. S13. Exposure of Cd/CB causes dose-dependent interstitial fibrosis in mice. Mice (n=5 per group) were treated intratracheally with Sal, $CdCl_2$ and/or CB. Mice lungs and BALF were collected at day 3, 7, 14, 21 and 28. Each dot represents an individual mouse. (**A**) Cd contents by ICP-MS from lung tissues. (**B**) Representative lung histology with collagen-1 staining at day 14. Scale bars, 100 μM. (**C**) DAB staining density from (**B**) was quantified. (**D**) SMI in Sal or $CdCl_2$ (0.16 mg/kg)-treated mice. SMI was calculated as published (*56*). Hydroxyproline content at (**E**) different concentration of $CdCl_2$, (**F**) different time points after $CdCl_2$ (0.16 mg/kg), (**G**) different concentration of CB, or (**H**) a combination treatment of $CdCl_2$ (0.16 mg/kg) and/or CB (5.0 mg/kg) at day 14. (**I**) Total number of BALF cells or (**J**) different cell types at different treatments. (**K**) Deposition of CB particles in BALF macrophages from Sal or Cd/CB-treated mice as detected by TEM and (**L**) the higher

magnification of inset from (**K**). Open arrow indicates the particles. Data shown are representative of experiments from Sal (n=5) and Cd+CB (n=5). Scale bars, 500 nM. (**M**) Quantification of CB positive macrophages from BALF as detected by TEM. Twenty five macrophages for each subjects were counted for quantification. * $P < 0.05$; ** $P < 0.01$; *** $P < 0.001$ using one-way ANOVA followed by Tukey's post-hoc analysis for (**A**) and (**C**) to (**J**) and two-tailed *t* test for (**M**).

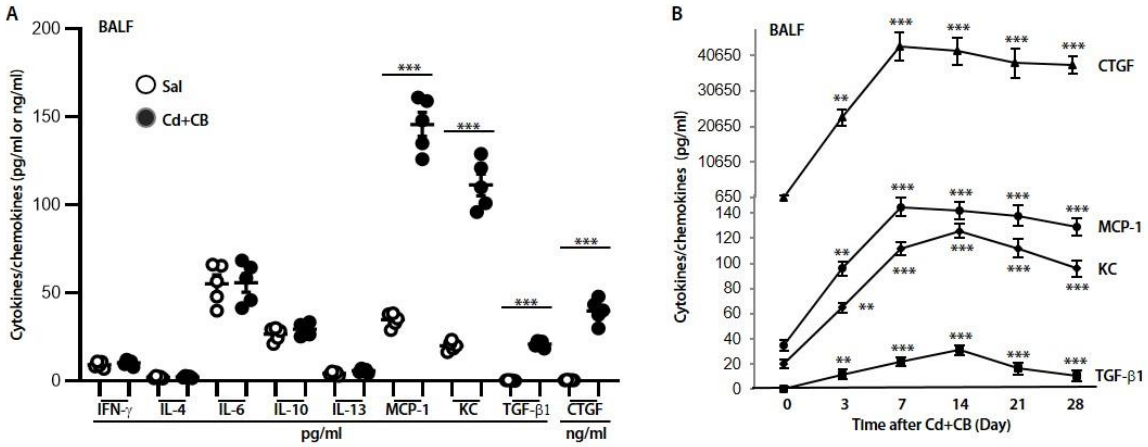

Fig. S14. Exposure of Cd/CB induces cytokine/chemokine secretion. Mice (n=5 per group) were treated intratracheally with Sal or $CdCl_2$ (0.16 mg/kg) plus CB (5.0 mg/kg) and BALF were collected at day 3, 7, 14, 21 and 28. Each dot represents an individual mouse. ELISA for cytokines/chemokine in BALF at (**A**) day 7 or (**B**) different time points. ** $P < 0.01$; *** $P < 0.001$ vs Sal control or day 0 using one-way ANOVA followed by Tukey's post-hoc analysis.

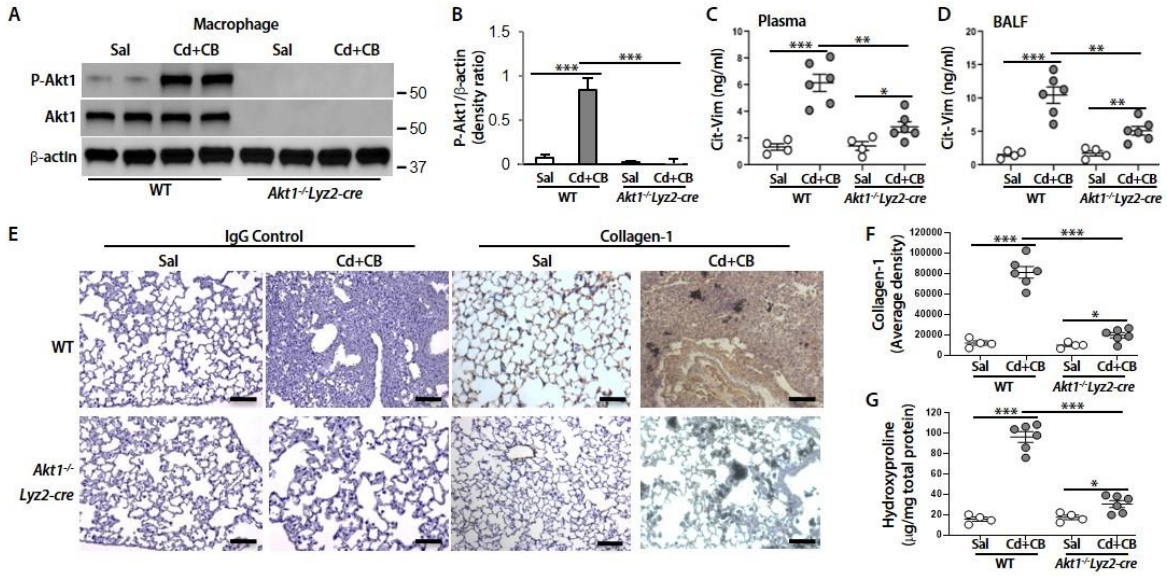

Fig. S15. Cd/CB-induced Vim citrullination and lung fibrosis are dependent on the activation of Akt1. (**A**) Immunoblot analysis in lung macrophages from WT (Sal, n=4; Cd+CB, n=6) and *Akt1*$^{-/-}$*Lyz2-cre* mice (Sal, n=4; Cd+CB, n=6) treated with Sal or $CdCl_2$ (0.16 mg/kg) plus CB (5.0 mg/kg). (**B**) Quantification of P-Akt1 from (**A**) (n=3). Cit-Vim amounts by ELISA in (**C**) plasma and (**D**) BALF at day 14 after mice exposure. (**E**) Representative lung histology with collagen-1 staining at day 14 and (**F**) DAB staining density from (**E**) was quantified. Scale bars, 100 μM. (**G**) hydroxyproline content at day 14. Each dot represents individual mouse. * $P < 0.05$; ** $P < 0.01$; *** $P < 0.001$ using one-way ANOVA followed by Tukey's post-hoc analysis.

Table S1. Demographics and baseline characteristics of subjects with IPF. Age (y; mean ± SD); [a] Smoker: Current or former smokers with at least a five pack-year smoking history; FVC (%): % of predicted, mean ± SD; DLCO (%): % of predicted, mean ± SD.

	Cohort 1 (Lung tissue)			Cohort 2 (Plasma sample)		
	Control	IPF	*P* value	Control	IPF	*P* value
Number	14	25	NA	57	84	NA
Age (y)	64 ± 9	65 ± 8	0.87	63 ± 11	67 ± 6	0.46
Gender (% male)	33	73	0.006	61	77	0.02
Race (% Caucasian)	87	100	0.08	93	91	0.33
Smoker (%) [a]	40	69	0.002	39	77	0.005
FVC (%)	85 ± 21	56 ± 15	1.95E-05	86 ± 15	63 ± 17	0.0001
DLCO (%)	82 ± 24	39 ± 12	2.23E-08	83 ± 10	44 ± 16	1.15E-05
Deaths (%)	NA	5	NA	NA	21	NA
Transplantations (%)	NA	1	NA	NA	5	NA
2-y transplant-free survival (%)	NA	28	NA	NA	31	NA

Table S2. Smoking status analysis of subjects with IPF. Smoker: Current or former smokers with at least a five pack-year smoking history; NS: Never smoker, S: Smoker; Age (y; mean ± SD); FVC (%): % of predicted, mean ± SD; DLCO (%): % of predicted, mean ± SD.

	Cohort 1 (Lung tissue)			Cohort 2 (Plasma sample)		
	NS	S	*P* value	NS	S	*P* value
Number	8	17	NA	19	65	NA
Age (y)	66 ± 8	63 ± 7	0.31	69 ± 10	65 ± 8	0.42
Gender (% male)	63	78	0.008	53	85	0.001
Race (% Caucasian)	100	100	1.00	84	91	0.19
FVC (%)	66 ± 15	52 ± 12	0.019	69 ± 16	57 ± 13	0.028
DLCO (%)	50 ± 14	35 ± 7.3	0.0025	52 ± 15	39 ± 9	0.006

Table S3. Accompanying fragmentation for the same peptide identified by IP-MS. Observed fragmentation: B+1H and B+2H ions highlighted in cyan; B-H2O, Y-NH3 and Y-H2O ions highlighted in yellow; Y+1H and Y +2H ions highlighted in magenta.

B	B+1H	B+2H	B-NH3	B-H2O	AA	Y+1H	Y+2H	Y-NH3	Y-H2O	Y
1	100.1	50.5			V	1705.8	853.4	1688.8	1687.8	14
2	229.1	115.1		211.1	E	1606.7	803.9	1589.7	1588.7	13
3	328.2	164.6		310.2	V	1477.7	739.4	1460.7	1459.7	12
4	457.2	229.1		439.2	E	1378.6	689.3	1361.6	1360.6	11
5	614.3	307.7	597.3	596.3	R+1	1249.6	625.3	1232.6	1231.6	10
6	729.3	365.2	712.3	711.3	D	1092.5	546.8	1075.5	1074.5	9
7	843.4	422.2	826.4	825.4	N	977.5	489.2	960.4	959.5	8
8	956.5	478.7	939.4	938.5	L	863.4	432.2	846.4	845.4	7
9	1027.5	514.3	1010.5	1009.5	A	750.3	375.6	733.3	732.3	6
10	1156.5	578.8	1139.5	1138.5	E	679.3	340.2	662.3	661.3	5
11	1271.6	636.3	1254.5	1253.6	D	550.3	275.6	533.2	532.3	4
12	1384.7	692.8	1367.6	1366.6	I	435.2	218.1	418.2		3
13	1531.7	766.4	1514.7	1513.7	M+16	322.2	161.6	305.1		2
14	1705.8	853.4	1688.8	1687.8	R	175.1	88.1	158.1		1